

Cell Reports, Volume 37

Supplemental information

Dual roles for piRNAs in promoting and preventing gene silencing in *C. elegans*

Brooke E. Montgomery, Tarah Vijayasarathy, Taylor N. Marks, Charlotte A. Cialek, Kailee J. Reed, and Taiowa A. Montgomery

Supplemental Figures

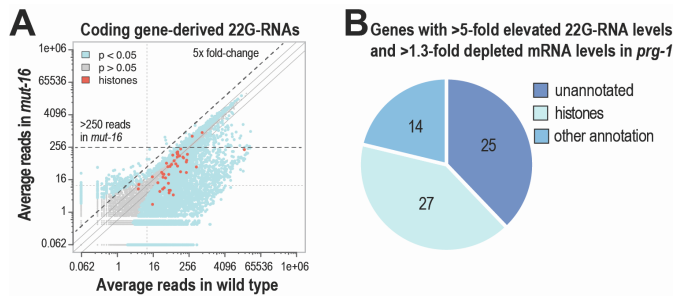


Figure S1. Gene classification of aberrant 22G-RNA targets in *prg-1* mutants. Related to Figure 1. (A) Scatter plot displaying each gene as a function of normalized \log_2 -transformed small RNA reads in wild type and *mut-16(pk710)* mutants. Note that the axes are reverse transformed to reflect non-transformed values. Hyperaccumulators were classified as genes that yielded an average of >250 normalized reads and which were upregulated >5 fold in *prg-1* mutants, as indicated by the dashed lines. Solid lines above and below the $y = x$ line indicate 2 and -2 fold-changes. Libraries are from dissected distal gonads ($n=3$ biological replicates for each strain). (B) Pie chart classifying genes that produced >5-fold as many 22G-RNA reads in *prg-1(n4357)* mutants compared to wild type and for which the corresponding mRNA was downregulated >1.3-fold.

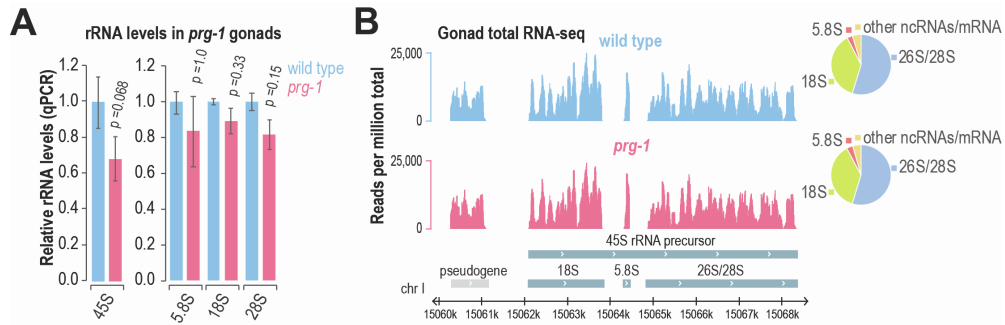


Figure S2. rRNA levels in *prg-1* mutants. Related to Figure 2. (A) Bar chart displaying mean relative rRNA levels in wild type and *prg-1*(*n4357*) mutant gonads, as determined by qRT-PCR. Error bars are standard deviation of the mean of 3 biological replicates. *rpl-32* or *act-1* levels were used for normalization. P values were calculated using two-sample t-tests and a Bonferroni correction was applied to account for multiple comparisons. (B) High-throughput sequencing read distribution across an rRNA locus (total RNA-seq from dissected gonads). One of three biological replicates for each strain is shown. The inset pie charts show rRNA and non-rRNA reads as a fraction of total reads. rRNA made up ~95% of all reads across each of the 6 libraries.

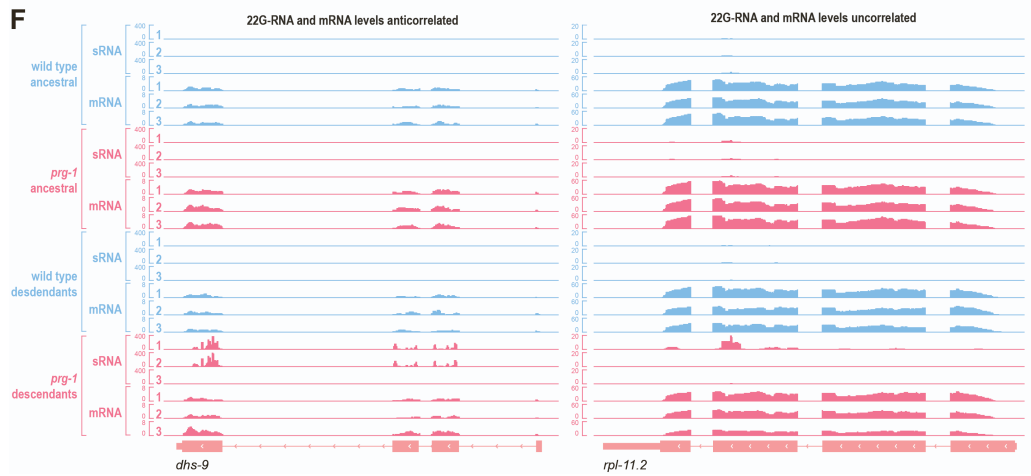
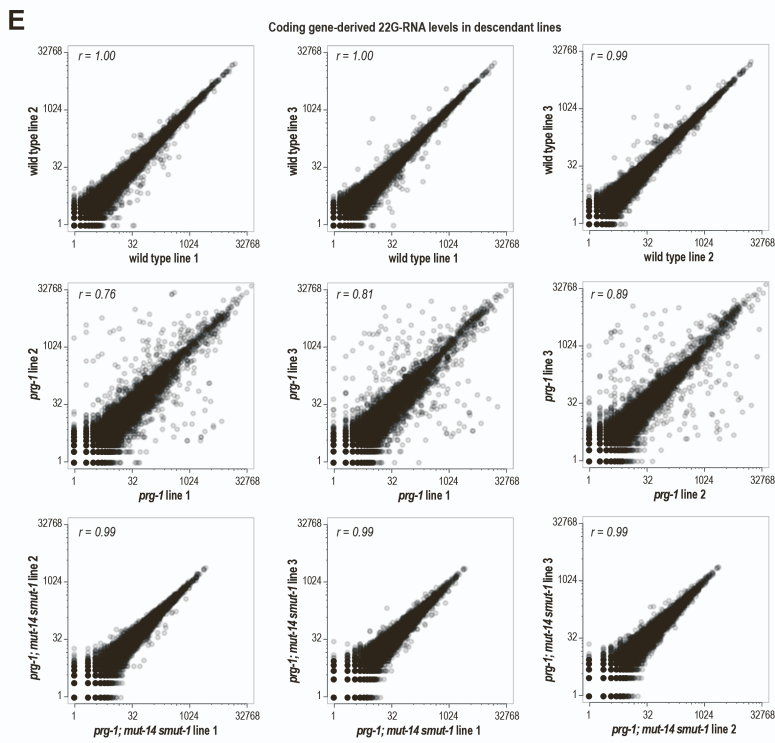
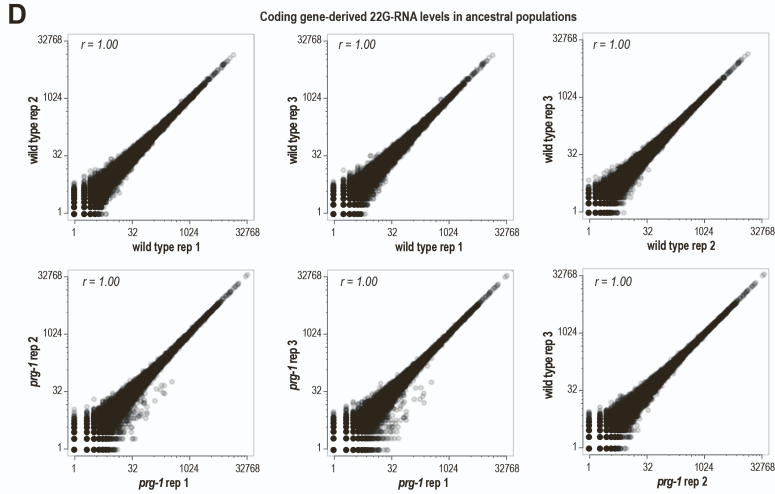
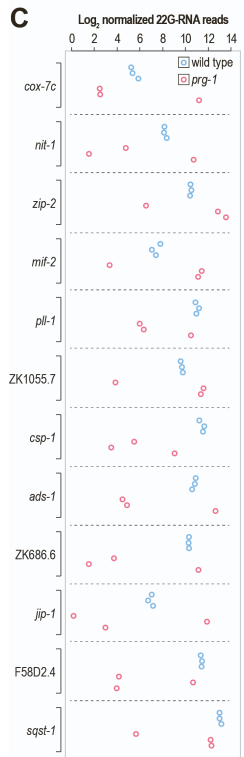
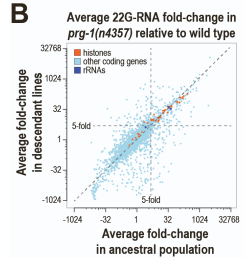
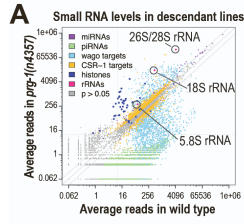


Figure S3. Widespread stochasticity in 22G-RNA production in *prg-1* mutants. Related to Figure 3. (A) Scatter plot displaying each small RNA feature colored by class as a function of normalized \log_2 -transformed high-throughput sequencing reads in wild type and *prg-1(n4357)* mutants at 50 generations of continuous growth (whole gravid adult animals, n=3 biological replicates for each strain). Note that the axes are reverse transformed to reflect non-transformed values. Solid lines above and below the $y = x$ line indicate 2 and -2 fold-changes. (B) Scatter plot displaying each coding gene and rRNA as a function of the \log_2 -transformed fold-change in *prg-1(n4357)* relative to wild type at 1 (ancestral population) and 50 generations (descendant lines) of continuous growth (axes show non-transformed values). Dashed lines mark $y = x$ and the 5 fold-change cutoff used to classify hyperaccumulators. (C) Plots displaying normalized \log_2 -transformed 22G-RNA reads for several genes in each wild type and *prg-1(n4357)* mutant line after 50 generations of continuous growth (y-axis shows \log_2 -transformed values). (D-E) Pairwise scatter plots comparing normalized \log_2 -transformed 22G-RNA reads for each coding gene across biological replicates from the ancestral population (D) or the descendant lines (E) of wild type and *prg-1(n4357)* (y-axis shows \log_2 -transformed values). *prg-1(n4357)*; *mut-14(mg464)* *smut-1(tm1301)* comparisons are shown as a control in (E). Pearson correlation values (r) are reported for non-transformed data (degrees of freedom = 20,474, $p < 2.2e-16$ for all comparisons). (F) mRNA and small RNA read distribution across representative gene loci, *dhs-9* and *rpl-11.2*. Three biological replicates or lines are shown for wild type and *prg-1(n4357)*.